ELSEVIER

Dramatic enhancement of wear stability in oil-enriched polymer gel nanolayers

Hyo-Sok Ahn [a], D. Julthongpiput [b], Doo-In Kim [a], V.V. Tsukruk [b,*]

[a] *Tribology Research Center, Korea Institute of Science and Technology, 39-1 Hawolgok-dong, Songbuk-gu, Seoul 136-791, South Korea*
[b] *Department of Material Science and Engineering, Iowa State University, 3053 Gilman Hall, Ames, IA 50011, USA*

Abstract

We report results on microtribological studies of chemically grafted, nanoscale polymer layers with enhanced wear stability. A 8–10 nm thick polymer gel layer composed of an elastomer was chemically grafted to a solid substrate and saturated with paraffinic molecules with different lengths of alkyl chains (15–24 carbon atoms, molecular weight $M = 212$–338). We studied the polymer layer ability to adsorb and held these paraffinic oils and considered to what extent the evaporation rate can be controlled by initial saturation and slower diffusion of longer alkyl chains. A microtribometer and a friction force microscope were used to accumulate the frictional characteristics and to study wear stability of the polymer layers. We observed that the presence of shorter chain paraffinic oil ($C_{15}H_{32}$ and $C_{18}H_{38}$) resulted in a lower value of the friction coefficient and higher wear resistance as compared to a dry polymer layer and a polymer gel layer with longer-chain paraffinic oil ($C_{20}H_{42}$ and $C_{24}H_{50}$). The approach of trapping mobile lubricants within a compliant nanoscale surface layer could lead to exceptionally robust molecular lubrication coatings for complex surface topography with developed nanosized features.
© 2003 Elsevier Science B.V. All rights reserved.

Keywords: Boundary lubrication; Paraffinic oil; Nanocomposite coatings; Microtribological properties

1. Introduction

Modern developments in high-density storage technologies and microelectromechanical systems (MEMS) have invigorated attempts to use ultrathin organic layers as protective/lubrication molecular coatings [1,2]. Ultrathin polymer films, Langmuir–Blodgett (LB) monolayers and multilayers, nanocomposite molecular layers, and self-assembled monolayers (SAMs) were explored as molecular lubricants aimed on the modification of the interfacial properties on the nanoscale [3,4]. Molecular lubricants with an ultimate thickness <100 nm are sought to provide reduced surface energy, low shear modulus and friction coefficient, and tailored dynamic behavior, along with the ability to self repair, sustain variations of temperature and humidity, and have long shelf-life [5]. It was demonstrated that, indeed, complex molecular coatings such as grafted supramolecular polymers, dendrimers, self-assembled multilayer films, and liquid-crystalline monolayers can dramatically change interfacial properties and behave very differently under severe space constraints [6,7].

In a previous study, we reported the fabrication of a robust molecular lubrication layer from a tri-block copolymers tethered to a solid surface [8]. A functionalized block-copolymer was chemically grafted to a silicon oxide surface and possessed lower adhesion and friction. Its tribological performance was enhanced by adding a minute amount of alkyl-chain paraffinic oil ($C_{15}H_{32}$). Although, paraffinic oil evaporated from the polymer films, a minute amount of oil was trapped within the grafted polymer layer. This resulted in a significant reduction of the local friction forces, surface adhesion, and an increase of the wear stability as reported in the previous publications [9,10].

Longer-chain paraffinic oils are considered here to enhance tribology performance via reducing oil phase mobility and crystallization at room temperature. We choose four alkyl-chain molecules with a number of carbons from 15 to 24 and studied the swelling rate, evaporation kinetics, and diffusion processes (Table 1). We focus on the friction response and the wear stability of these nanoscale polymer gel layers using a combination of micro- and nanotribology studies with Auger electron spectroscopy (AES) that allows quantitative surface chemical analysis [11].

2. Experimental

As a nanocomposite polymer layer, we used poly[styrene-b-(ethylene-co-butylene)-b-styrene] (SEBS) with Mn =

* Corresponding author. Tel.: +1-515-294-6904; fax: +1-515-294-5444.
E-mail address: vladimir@iastate.edu (V.V. Tsukruk).

Table 1
Chemical formula, molecular weight, and melting point of different paraffinic oils

Paraffinic oil	Chemical formula	Formular weight (g/mol)	Melting point (°C)
Pentadecane	$C_{15}H_{32}$	212	9.9
Octadecane	$C_{18}H_{38}$	254	29
Eicosane	$C_{20}H_{42}$	282	37
Tetracosane	$C_{24}H_{50}$	338	50

41,000 g/mol, Mw/Mn = 1.16. SEBS copolymer was Kraton 1901 (Shell) with styrene and maleic anhydride (MA) functional group content of 29 and 2 wt.%, respectively [12]. The paraffinic oils, $C_{15}H_{32}$–$C_{24}H_{50}$, (Aldrich) were used as lubrication additives (Fig. 1, Table 1). The grafted dry polymer layers were fabricated on the (1 0 0) silicon wafer according to the procedure published earlier [12,13]. For annealing, the dry polymer layer was placed in a vacuum oven
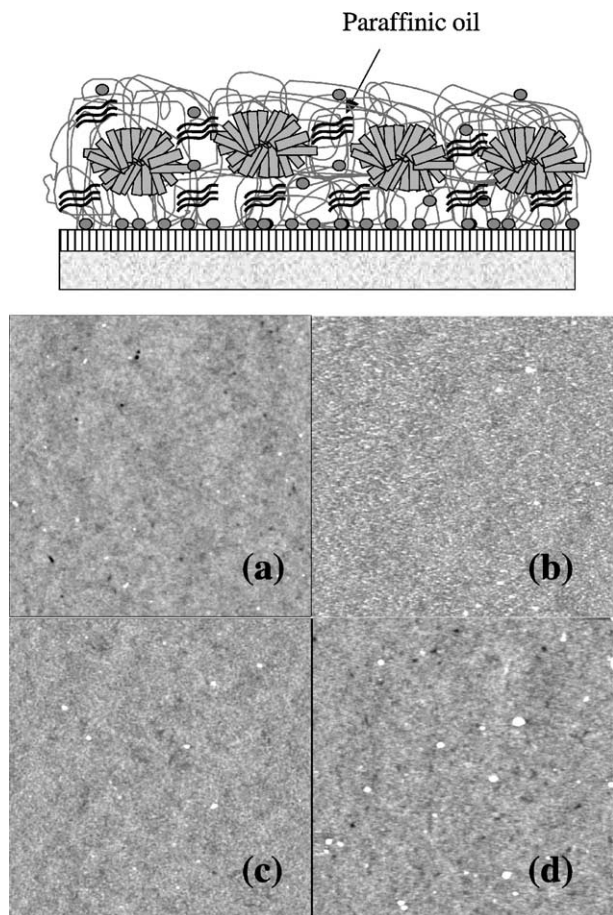

Fig. 1. (Top): microstructure of grafted SEBS layer grafted to epoxy-terminated surface. Hard blocks are presented by gray spheres and the soft rubber matrix contains anchoring groups shown by gray dots. The paraffinic molecules entrapped in the rubber matrix of the SEBS layer are shown by black curves. (Bottom): (a) SPM topographical images of the dry polymer layers; (b–d) polymer gel layer saturated with C15, C20, and C24 oils, respectively. Scan size is 10 μm × 10 μm, height scale is 30 nm, light tapping mode.

at 60 °C for 24 h. For oil treatment, the dry polymer layers were placed in a sealed tube and kept for saturation with oil vapor at 60 °C for 24 h. The diffusion coefficient and the rate of evaporation were evaluated with microbalances and ellipsometry according to the procedure described in our previous publication [14]. Characterization of the polymer gel layers was conducted within several months after fabrication to allow complete equilibration and evaporation of unbounded oil from the polymer surfaces.

A custom-built microtribometer, an oscillating friction and wear tester, was used to accumulate the frictional characteristics and to study wear stability of the polymer layers in a reciprocation mode according to the procedure described earlier [14]. The 3 mm diameter steel ball with a smooth surface (microroughness <10 nm) was mounted in a carrier head and was oscillated against a stationary planar specimen with an applied load of 0.3 and 1.8 N, which corresponded to the maximum Hertzian pressure of 300 MPa and 1.2 GPa, respectively. Sliding speed was 4.43 mm/s, a stroke length was 3 mm, and a number of cycles tested reached 20,000.

The surface microstructure was investigated with Auger electron spectroscopy and scanning probe microscopy (SPM). AES surface analysis was performed on a PHI-670 microscope using a field emission gun with an accelerating voltage of 5 kV and a current of 0.0211 μA. The working potential for depth sputtering was 1 kV using Ar-ion. Under this working condition, the sputtering rate was about 0.5 nm/min when calibrated against SiO_2. SPM was done on a Dimension 3000 (Digital Instruments Inc.) microscope according to the known procedure [12,13]. We used the tapping mode (amplitude and phase modes) to reveal surface morphology and microstructure. The contact mode was used to observe microstructure and friction properties under higher normal forces. Friction forces were evaluated from SPM friction loops under different normal loads according to the procedure adapted in our lab [15]. A linear regression analysis was used to determine the friction coefficient from these data in accordance with the generalized Amonton's law approximation. We estimated vertical and torsional spring constants of SPM cantilevers by using their resonant frequencies and calibration plots proposed in our previous publication [16].

3. Results and discussions

3.1. Enrichment of polymer layers with alkyl-chain oils

Fig. 2 shows the swelling ratio $Y = W_t/W_0$ (W_0 is the initial weight of the dry polymer specimen and W_t the polymer weight at a certain time after immersion in oil) of bulk SEBS material as a function of time. The bulk polymer samples were immersed on oil at 60 °C for different periods of time. We observed that the bulk polymer specimens immersed in the short chain paraffinic oils ($C_{15}H_{32}$ and $C_{18}H_{38}$) reached equilibrium after 4 h and the longer-chain
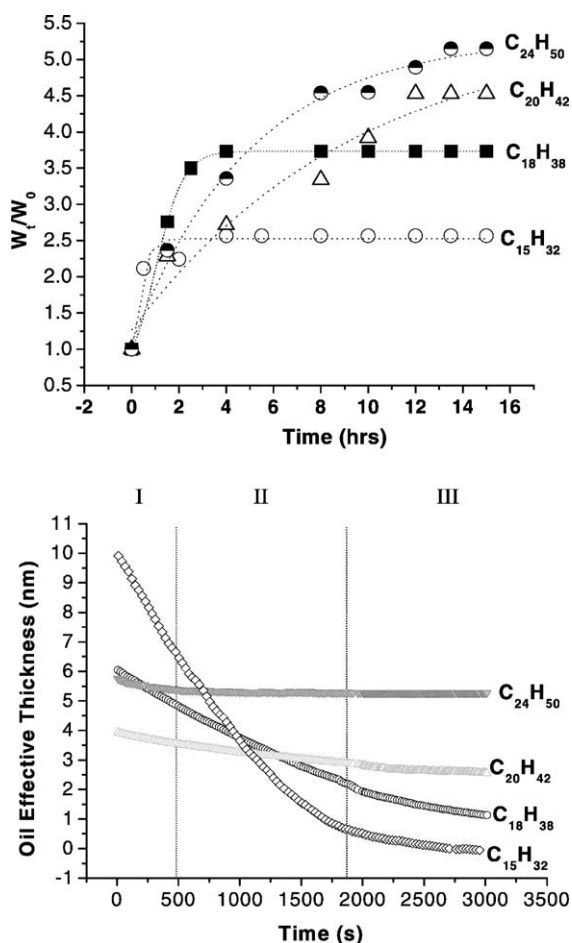
Fig. 2. (Top): time dependence of the polymer swelling ratio for bulk SEBS polymer submerged in oil, W_t/W_0. The dash line is a guide for an eye. (Bottom): the effective oil layer thickness d_t obtained for the grafted polymer gel layer from ellipsometry data according to the bilayer model [10].

oils ($C_{20}H_{42}$ and $C_{24}H_{50}$) saturated polymers after 15 h. The diffusion coefficient, D, of paraffinic molecules within the bulk polymer at 60 °C was calculated from the measurement of the swelling ratio as a function of time according to [17] (Table 2). For all oils, the swelling rate was very high at the early stage and became slower before the final equilibrium reached. As expected, the diffusion coefficient for longer-chain molecules is about one order of magnitude

Table 2
The diffusion coefficients of different paraffinic oils in polymer layer at 60 °C and the rate of oil evaporation from the grafted polymer layers at different stages (see Fig. 2)

Paraffinic oil	Diffusion coefficients (cm^2/s)	Evaporation rate (g/m^2 s)		
		I	II	III
$C_{15}H_{32}$	1.01E-3	5.2E-6	3.4E-6	4.3E-7
$C_{18}H_{38}$	8.71E-4	1.8E-6	1.6E-6	8.0E-7
$C_{20}H_{42}$	7.15E-4	6.0E-7	4.0E-7	2.0E-7
$C_{24}H_{50}$	5.42E-4	5.0E-7	4.0E-8	2.0E-9

lower than that of short-chain molecules. The highest oil up-take in the polymer was observed for $C_{24}H_{50}$ with more than five times mass increase. These preliminary studies lend support to the original hypothesis that paraffinic oils are compatible to the rubber, polyethylene-like PEB block of SEBS, which results in the polymer gel formation [10,18].

Another important property we tested was the evaporation rate. The kinetics of oil evaporation from the grafted polymer gel layer as measured by ellipsometry is shown in Fig. 2. All plots show three different regimes as was discussed in detail in previous publication [10]. Table 2 shows the rate of oil evaporation from the grafted polymer layer at different stages: (i) surface diffusion, (ii) swollen polymer matrix diffusion, and (iii) diffusion of residual alkyl molecules inside the grafted polymer gel layer [10]. It appears that the short-chain paraffinic oil, C15, gradually evaporated from the polymer film with only some residual effective oil layer <1 nm left in the films. The overall evaporation rate is much lower for longer-chain molecules (Table 2), e.g. for C24 molecules, the rate of evaporation was 4.0×10^{-9} g/m^2 s. This value is over three orders of magnitude lower than that for C15 (3.0×10^{-6} g/m^2 s) and a free oil surface (6.7×10^{-5} g/m^2 s) as reported in the previous publication [10,14]. This indicated that the mobility of the longer alkyl molecules was severely restricted when they were trapped within the rubber matrix grafted to the silicon substrate.

3.2. Surface microstructure and chemical composition of polymer gel layer

The grafted polymer films possess uniform, smooth, and homogeneous surface with only a few aggregates observed over surface areas of 10 μm across as illustrated in Fig. 1 (microroughness of 0.2–0.4 nm within 1 μm^2 area was measured for all polymer layers). For polymer layers exposed to long-chain oils, scarce globular aggregates were observed. The highest surface concentration of aggregates was observed for the highest molecular weight paraffinic oil, C24. The lateral size of surface aggregates is within 400–500 nm. Larger aggregates, up to several microns across were observed on SEM images (Fig. 3a). Obviously that this is related to the crystallization process of paraffinic oil with higher melting points during cooling from 60 °C to room temperature that results in the formation of microscopic paraffinic crystals. Indeed, optical microscopical analysis of similar paraffins (mp 48–49 °C) in crossed polarizers shows many fine "crystals" with random orientation after crystallization from melt [19]. These crystals are composed of many overlapping thin prismatic lamellae with lateral sizes from several hundred nanometers to several microns.

AES data demonstrated the polymer layer was predominantly composed of carbon atoms (main component of polystyrene, rubber blocks, and paraffinic oil) with detected tracks of oxygen (MA groups, epoxy groups, and a silicon dioxide layer) and a silicon substrate (Fig. 3(b)). The depth profiles of the different elements within the polymer gel
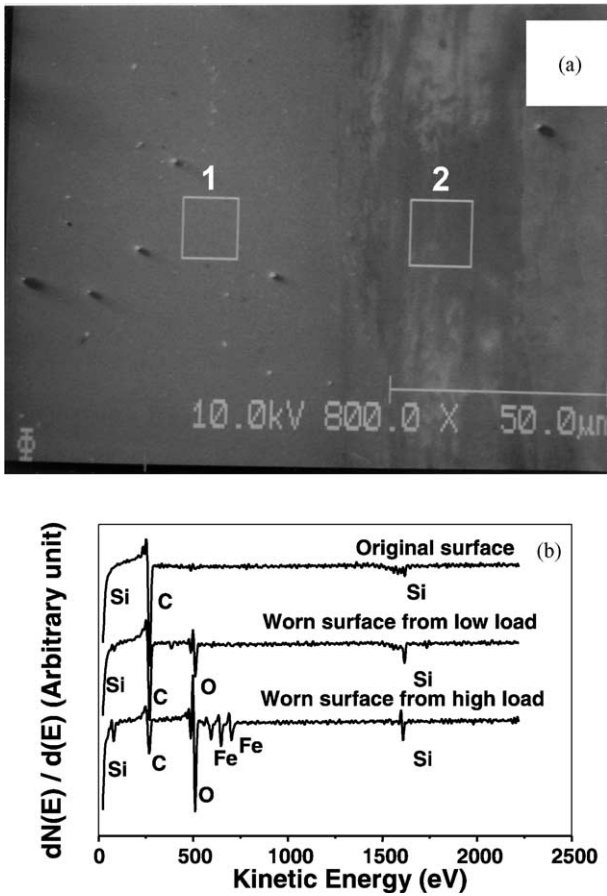
Fig. 3. (a) SEM image of polymer gel layer with C18 oil with a wearing trace under a low load (0.3 N). Boxes mark the surface areas for AES analysis performed for original (1) and partially worn (2) areas. (b) AES spectra of the original and worn surfaces areas.

layers exposed to different paraffinic oils are presented in Fig. 4. The polymer gel layer exposed to C20 molecules shows higher carbon contain. There were no significant differences in the depth profiles of all elements in the polymer layers exposed to other oils. The layer thickness roughly estimated from AES data calibrated against silicon was about 8 nm that was close to 9 nm value obtained from ellipsometry. These findings imply that their initial microstructures are similar for all polymer gel layers and consistent with the results presented in our earlier publication for C15 molecules [10].

3.3. Friction behavior and wear stability of the polymer layers

SEM image of polymer gel layer with C18 oil exposed to rubbing with a steel ball at 0.3 N normal load shows a weak wear track (Fig. 3(a)). An increase of silicon and oxygen elements was detected by AES for these partially worn areas (Fig. 3b). This implied that the polymer gel layer might be partially oxidized and deformed. Indeed, depth profiling of various elements shows decreasing content of carbon and a sharp increase of oxygen (Fig. 5). This confirms that the increase of oxygen content within the worn topmost surface layer was caused by the oxidation of the metal surfaces, oxidation and decomposition of the organic molecules from the surface lubricant layer [15,20]. In addition, sputtering time was much shorter for the worn layer, which indicated its highly compressed state with a thickness not exceeding 4 nm. There were differences in the depth profile of oxygen and carbon elements among the polymer gel layers of the worn surfaces. For example, the polymer gel layer with C18 displayed higher carbon content than the polymer gel layers
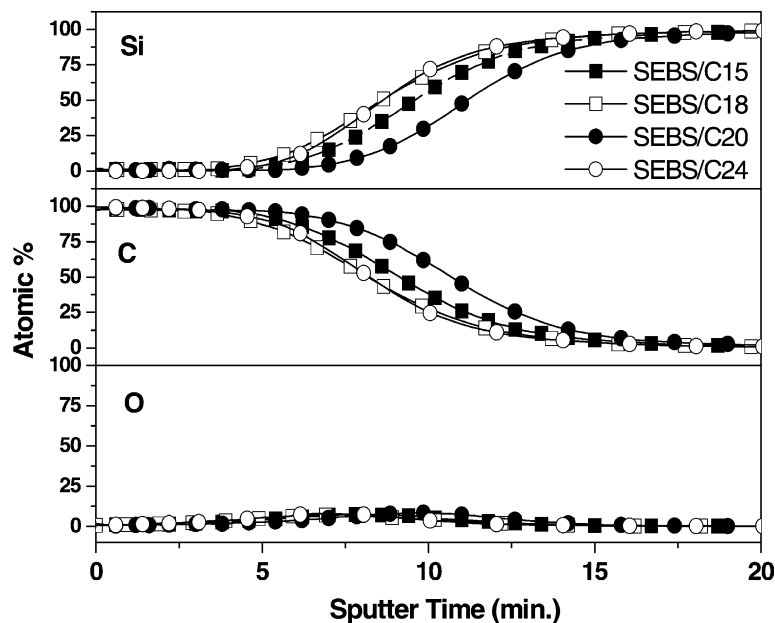

Fig. 4. AES results for the depth profiles of difference chemical elements for various polymer gel layers.
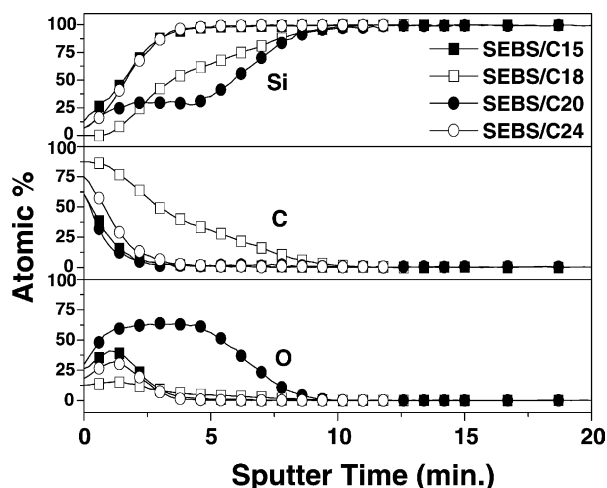
Fig. 5. AES results for the depth profiles of difference chemical elements for partially worn surfaces of various polymer gel layers.

with C15, C20, and C24 and layer with C20 shows much higher oxygen concentration (Fig. 5). These variations can be due to occasional presence of surface aggregates and exposed silicon dioxide surface or debris.

AES analysis of the polymer gel layer saturated with C18 exposed to a high normal load showed that iron, silicon, and oxygen became dominant elements within the worn area (Fig. 3b). Apparently, iron was present on the silicon surface due to material transfer from the counterpart steel ball to the worn surface during ultimate local damage of the silicon substrate and these AES data are entirely consistent with previously published data for the similar film studied in [9].

Fig. 6 shows the coefficient of friction calculated from microtribological data as a ratio of the lateral forces to the normal load as a function of the number of sliding cycles. At a low normal load of 0.3 N, the grafted polymer gel layers exposed to oils, showed a performance much better than the uncoated silicon and the dry polymer film. The polymer gel layers did not show a failure or significant deterioration up to 20,000 cycles (the maximum number of cycles tested here) whereas the bare silicon and the dry polymer layer failed within 200 and 2700 cycles, respectively (both values were averaged over three independent measurements).

The polymer gel layers with short chain (C15) paraffinic oil showed the lowest friction coefficient among the layers (~0.05). The friction coefficient increased with the increasing molecular weight of paraffinic oils to 0.11–0.12 for the polymer gel layer with C24. The friction coefficient value reached the highest value of 0.13–0.17 for the dry polymer layer and a bare silicon substrate (Fig. 6). The effect of paraffinic oil on the frictional behavior of the polymer layer became more significant for longer runs when the dry polymer layer finally started to deteriorate. At a higher normal load of 1.8 N, the dry polymer failed only after 250 cycles while the polymer gel layers were stable up to 500–700 cycles (C20–C24) and 900–1000 cycles (C15 and C18).
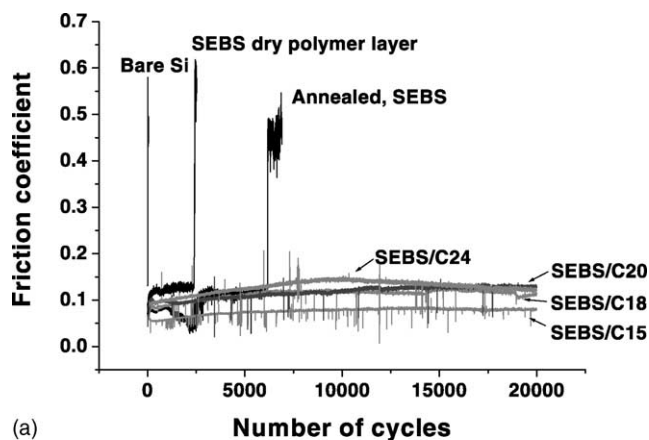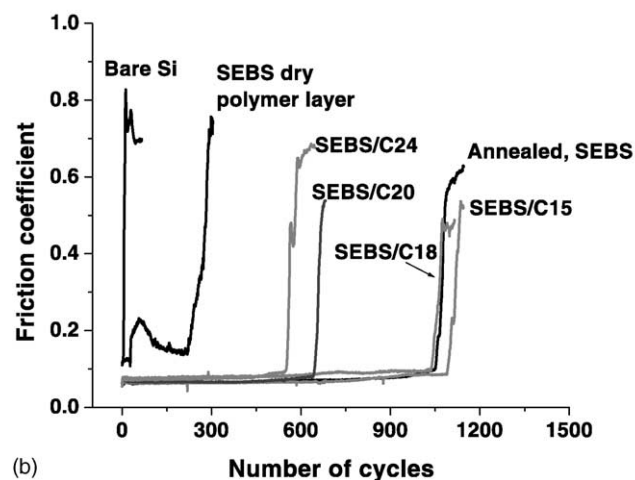
Fig. 6. The coefficient of friction as a function of a number of sliding cycles for the bare silicon, dry polymer layer, annealed polymer layer, and polymer gel layers at the normal load of 0.3 N (a) and 1.8 N (b).

It is worth noting that additional annealing of the polymer layer at 60 °C for 24 h also resulted in significant improvement of wear resistance, especially under high normal load (Fig. 6). Obviously that additional annealing of the polymer layer allowed MA functional groups of the rubbery block poly(ethylene-co-butylene) to react with the epoxy groups of the supporting surface, thus, resulting in a stronger adhered layer. However, the presence of alkyl-chain molecules is still more important factor in enhanced wear resistance at low normal loads (Fig. 6a).

Finally, the nanotribological properties were characterized with friction force microscopy (Fig. 7). Loading curves were obtained for a bare silicon substrate, annealed polymer layer, and the oil-exposed polymer layers under identical conditions (identical probe, scanning velocity, scanning size, and the range of normal loads). The friction coefficients calculated as a slope of a linear approximation were determined to be the lowest for polymer layers with C15 and C18 oils. The friction coefficient for their layers decreased to 0.02, which was much lower than that for the silicon substrate (0.07–0.1). Despite the fact than the absolute
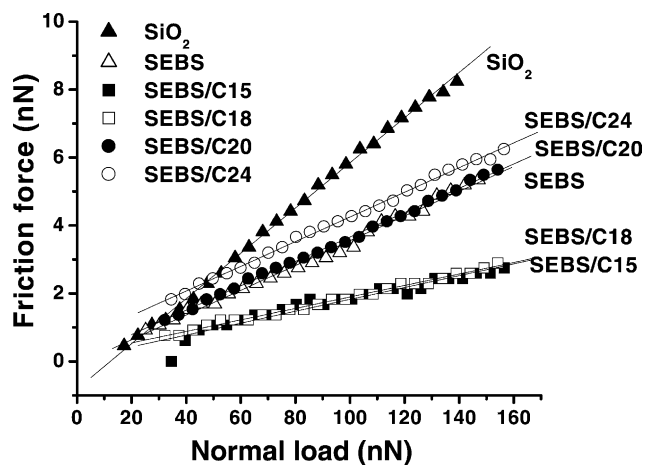
Fig. 7. Friction forces vs. normal loads as measured for the bare silicon, dry polymer layer, annealed polymer layer, and polymer gel layers with paraffinic oil (C15–C24).

values of the friction coefficient calculated from SPM data were systematically lower than those determined with the microtribotester, general trends were very consistent. Hence, we can conclude that the polymer gel layer treated with C15 and C18 paraffinic molecules showed the best tribological performance.

4. General conclusions and discussion

We report the friction response and the wear stability of the uniform, smooth, and homogeneous polymer gel layer grafted on a silicon surface and saturated with paraffinic molecules with different lengths of alkyl chains (15–24 carbon atoms). We observed that the presence of shorter chain paraffinic molecules ($C_{15}H_{32}$ and $C_{18}H_{38}$) resulted in a lower value of the friction coefficient and higher wear resistance as compared to a dry polymer layer and a polymer gel layer saturated with longer-chain paraffinic oil ($C_{20}H_{42}$ and $C_{24}H_{50}$).

Hence, we can conclude that shorter chain molecules improve the lubrication properties of the tethered polymer layers, resulting in the lowest value of the friction coefficient. This phenomenon can be understood considering known theories, which relate a quality of solvent and resulting osmotic pressure [21]. As was demonstrated, higher osmotic pressure between grafted polymer chains shows up in the good solvent, which allows supporting a larger normal load. In addition, the frictional forces between compressed, rubbing solid surface may be dramatically reduced while shorter chain paraffinic molecules retaining a fluid interfacial layer, preventing significant interpenetrate and reducing lateral forces requiring to slide them [22]. The coupling between the large normal compression sustained and a fluid interfacial region is the origin of the good lubrication properties of grafted polymer layers solvated by a good solvent [22]. Using a

better solvent for a given polymer layer reduces the friction coefficient relative to a less good solvent [23]. The Flory–Rehner theory defines the best solvent as the one with the closest solubility parameter [24]. Since the shorter chain paraffinic oils possess solubility parameters close to PEB segments, they are expected to be better solvents than the longer-chain molecules [25].

These results may have some important technological applications since the durability of the organic ultrathin polymer surface films has been concerned. The most common case, low molecular weight lubricant is removed and evaporates from the protective layers, result to wear off when operated under high pressure [26]. On the other hand, the redistribution of fluid lubricant materials occurs on surface with complex topography such as sharp ridges is a critical issue under long-range storage conditions. Thus, it may be possible to make ultrathin interfacial polymer layers (<5–10 nm) uniformly distributed over textured surfaces with ability to adsorb and held short-chain paraffinic molecules and support large pressures while operated under high-pressure conditions. This approach alone or in a combination with a hard capping layer in trilayer nanoscale coatings [27,28] could lead to exceptionally robust molecular lubrication coatings for complex surface topography of MEMS devices.

Acknowledgements

References

[1] R.S. Muller, in: B. Bhushan (Ed.), Micro/Nanotribology and Its Applications, Kluwer Academic Publishers, Dordrecht, The Netherlands, 1997, p. 579.
[2] C.M. Mate, J. Wu, Nanotribology of polymer surfaces for disk drive applications, ACS Symp. Ser. 741 (2000) 405.
[3] M.T. Dugger, D.C. Senft, G.C. Nelson, Friction and durability of chemisorbed organic lubricants for micro-electromechanical systems, ACS Symp. Ser. 741 (2000) 428.
[4] A. Ulman, Introduction to Ultrathin Organic Films, Academic Press, San Diego, CA, 1991.
[5] V.V. Tsukruk, Molecular lubricants and glues for micro- and nanodevices, Adv. Mater. 13 (2) (2001) 95–108.
[6] J. Israelachvili, Intermolecular and Surface Forces, Academic Press, San Diego, CA 1992.
[7] A.W. Adamson, Physical Chemistry of Surfaces, Wiley, New York, 1990.
[8] I. Luzinov, D. Julthongpiput, V. Gorbunov, V.V. Tsukruk, Nano-tribological behavior of tethered reinforced polymer monolayers, Tribology Int. 34 (2001) 327–333.
[9] A. Sidorenko, D. Julthongpiput, I. Luzinov, V.V. Tsukruk, Oily nanocoatings, Tribol. Lett. 13 (2) (2002) 101–104.

[10] D. Julthongpiput, A. Sidorenko, H. Ahn, D. Kim, V.V. Tsukruk, Towards self-lubricated nanocoatings, Tribol. Int. 35 (2002) 829–836.

[11] D.T.L. van Agterveld, S.A. Koch, G. Palasantzas, J.T.M. De Hosson, Surf. Sci. 482–485 (2001) 254–259.

[12] V.V. Tsukruk, Scanning probe microscopy of polymer surfaces, Rubber Chem. Tech. 70 (1997) 430–475.

[13] I. Luzinov, D. Julthongpiput, V.V. Tsukruk, Stability of microdomain morphology in tethered block-polymer monolayers, Polymer 42 (2001) 2267–2273.

[14] D. Julthongpiput, H. Ahn, D. Kim, V.V. Tsukruk, Tribological behavior of grafted polymer gel layer, Tribol. Lett. 13 (2002) 35–40.

[15] V.V. Tsukruk, V.N. Bliznyuk, J. Hazel, D. Visser, M.P. Everson, Organic molecular films under shear forces: fluid and solid Langmuir monolayers, Langmuir 12 (1996) 4840–4849.

[16] J. Hazel, V.V. Tsukruk, Friction force microscopy measurements: normal and torsional spring constants for V-shaped cantilevers, J. Tribol. 120 (1998) 814–819.

[17] A. Jha, A.K. Bhowmick, Influence of dynamic vulcanization and phase interaction on the swelling behavior of the thermoplastic elastomeric blends of nylon-6 and acrylate rubber in various solvents and oil, J. Appl. Polym. Sci. 69 (1998) 2331–2340.

[18] J.R. Quintana, E. Díaz, I. Katime, Physical gelation of SEBS in several paraffinic oils, Polymer 39 (1998) 3029–3034.

[19] C. Pawlowski, Transformation of paraffin under the influence of a-particles, J. Chim. Phys. 27 (1930) 266–276.

[20] S.M. Hsu, Boundary lubrication: current understanding, Tribol. Lett. 3 (1997) 1–11.

[21] U. Raviv, R. Tadmor, J. Klein, Shear and frictional interactions between adsorbed polymer layer in a good solvent, J. Phys. Chem. B 105 (2001) 8125–8134.

[22] J. Klein, Shear, friction and lubrication forces between polymer-bearing surface, Ann. Rev. Mater. Sci. 26 (1996) 581–612.

[23] L. Mandelkern, P.J. Flory, The frictional coefficient for flexible chain molecules in dilute solution, J. Chem. Phys. 20 (2) (1952) 212–214.

[24] G.M. Bristow, W.F. Watson, Viscosity-equilibrium swelling correlations for natural rubber, Trans. Faraday Soc. 54 (1958) 1731–1742.

[25] D.R. Lide (Ed.), in: Polymer Handbook, fourth ed., Wiley, Canada, 1999, pp. 698–704.

[26] T.E. Karis, B. Marchon, V. Flores, M. Scarpulla, Lubricant spin-off from magnetic recording disks, Tribol. Lett. 11 (3/4) (2001) 151–159.

[27] V.V. Tsukruk, A. Sidorenko, H. Yang, Polymer nanocoatings with non-linear elastic response, Polymer 43 (2002) 1650–1695.

[28] V.V. Tsukruk, H.-S. Ahn, A. Sidorenko, D. Kim, Triplex molecular layers with nonlinear nanomechanical response, Appl. Phys. Lett. 80 (2002) 4825–4827.